A 100 keV NEUTRAL LITHIUM BEAM FOR PLASMA DIAGNOSTICS

M. Kick, K. Mc Cormick, H. Schmid

IPP 2/265 January 1983

MAX-PLANCK-INSTITUT FÜR PLASMAPHYSIK

8046 GARCHING BEI MÜNCHEN

MAX-PLANCK-INSTITUT FÜR PLASMAPHYSIK

GARCHING BEI MÜNCHEN

A 100 keV NEUTRAL LITHIUM BEAM FOR PLASMA DIAGNOSTICS

M. Kick, K. Mc Cormick, H. Schmid

IPP 2/265 January 1983

Die nachstehende Arbeit wurde im Rahmen des Vertrages zwischen dem Max-Planck-Institut für Plasmaphysik und der Europäischen Atomgemeinschaft über die Zusammenarbeit auf dem Gebiete der Plasmaphysik durchgeführt.

IPP 2/265

M. Kick
K. Mc Cormick
H. Schmid

A 100 keV neutral lithium beam for plasma diagnostics

January 1982 (in English)

Abstract

For measurements of the poloidal magnetic field of toroidally confined plasmas a gun has been developed which can produce a neutral lithium beam with energies up to 100 keV. At 100 keV a neutral particle flux of 1.95×10^{16} sec^{-1} (equivalent beam current 3.1 mA) with a FWHM of 0.8-1.2 cm at a distance of 210 cm from the neutralizer is achieved, the peak neutral particle flux density being about $2 \times 10^{16} cm^{-2} sec^{-1}$. Using a solid ion source (β-Eucryptite) the ion beam is formed in a pulsed two-stage electrostatic extractor-accelerator system and neutralized in a charge-exchange cell utilizing either lithium or sodium. On Wendelstein VII-A the beam was pulsed on for about 2 seconds with a duty cycle of ≥ 30 sec.

The dependence of the beam intensity (number of particles per second and cm^2) on various parameters is investigated for an energy of 97 keV. Hereby, only single parameter variations around one particular set of "optimum" values are considered.

1. INTRODUCTION

The feasibility of determing the poloidal magnetic field of Pulsator by measuring the direction of polarization of the collisionally induced lithium-resonance-line has been demonstrated /1/. The lithium atoms were brought to the examined plasma volume via a neutral lithium beam with an energy of 6 keV and a maximum intensity of ~ $6 \times 10^{13} sec^{-1} cm^{-2}$. The intensity and energy of the beam proved to be too small to allow other than proof-of-principle measurements: the S/N-ratio of the detected light signal suffered both as a result of the low beam intensity and inadequate beam penetration for peak densities above $2 \times 10^{13} cm^{-3}$. Estimates based on measured or calculated cross-sections for the involved scattering processes indicated that an energy of about 100 keV should enable the beam to sufficiently penetrate plasmas with peak electron densities of $\gtrsim 10^{14} cm^{-3}$ /2/ (at least for the case $Z_{eff} = 1$). Therefore the development of a lithium beam with energies in the range of 100 keV and intensities of ~ $10^{16} sec^{-1} cm^{-2}$ was started.

2. THE LITHIUM GUN

The lithium gun consists of an emitter, an extractor, an electrostatic lens to accelerate and focus the extracted ions, and a charge-exchange cell in which the beam is neutralized.

2.1 ION SOURCES

A ceramic, β-Eucryptite, was chosen as the ion source. This material is capable of emitting several mA/cm^2 of lithium ions under the influence of an electric field, /3/ when heated to about $1400^{\circ}C$.

Two types of ion sources were tested. One was similar to that suggested by Möller and Kamke /4/. The other was a heavy duty version of the lithium emitter that is offered by Spectra-Mat Corp., of Watsonville, California /5/. Both sources are able to emit a lithium ion current of several mA/cm^2; both are subject to occasional burn-out when heated to temperatures up to $1400^{o}C$.

The Möller+Kamke-type of ion source is a flat spiral of 0.8 mm ø molybdenum-wire which is supported by a "crucible" of 16 mm ø and 3 mm depth. β-Eucryptite powder is filled into the "crucible" and melted by passing a current through the spiral. This procedure is repeated until the spiral is covered by a glassy surface of β-Eucryptite. The surface is bumpy, following the spiral wire.

The Spectra-Mat ion source consists of a molybdenum cylinder of about 15 mm ø and 13 mm height, on top of which a highly porous (70 % porosity) tungsten plug is welded. The system is heated by a helix of 1 mm ø molybdenum wire, which is potted into the cyclinder with high purity Al_2O_3. Although the source comes with a small amount of β-Eucryptite melted into the W-plug, this is not able to sustain the needed ion current. Therefore additional coatings were necessary: a thin layer of β-Eucryptite is melted into the W-plug by heating it to temperatures higher than $1450^{o}C$ (needed power ~ 200 Watts) under high vacuum conditions. This procedure, sometimes repeated ten or more times, is carried out until a smooth glassy surface covers the W-plug.

Because of the better reproducibility of the emitting surface, a Spectra-Mat ion source is used in the final version of the gun. One such well-prepared ion source was able to provide ions for about 4000 shots before recoating was needed. The duration of the pulses was about 1.5 seconds. The extracted current from the HV power supply was about 3 mA. This is an upper limit for the ion current, because secondary electrons produced along the beam path may flow back to the emitter thereby increasing the power supply current. Hence, an upper limit for the current drawn from this ion source is 5 mAh.

A second ion source provided about 1000 shots of about 2 seconds pulse length with about 6 mA extracted current. This correponds to a total current of 3.5 mAh before recoating was necessary.

2.2 THE ION OPTICAL SYSTEM

The ions are extracted from the source by an electrical field and accelerated and focussed by an electrostatic optical system. The first version of the extraction system consisted of an ion source in a Pierce-configuration /6/: The ion source was part of one spherical electrode; the extraction of the ions was done by a second sphere According to Pierce the "focal spot" of the beam can be varied in size and distance by varying the distance between the two spheres. This Pierce-extractor-geometry was followed by a three-stage accelerating-focussing-system consisting of three cylindrical tubes (Fig. 1).

Maximum intensities were achieved by connecting the extraction-sphere and the first tube , and grounding the second and third tubes. According to this result the third tube was removed. In addition, different electrode shapes were tested in the extraction stage: The spheres were replaced by cones with different slopes. Tubes of different lengths and diameters were tested.

The system that yielded maximum intensities is the following (Fig. 2): A Spectra-Mat ion source (ø 15 mm) is surrounded by a conical "Wehnelt" with an angular slope of 60° to the beam axis. The extractor consists of a second cone (slope angle 50°) with an extraction hole of 20 mm ø. The distance between the ion source and the "Wehnelt" on one hand and the extractor on the other can be varied. The first tube of 75 mm length and 65 mm diameter is attached to the extractor. A second tube of 100 mm length and 30 mm ø follows, forming an ion optical lens together with the first tube. The distance between the two tubes is variable.

For a beam energy of 100 keV the electrical potentials applied to the electrodes are as follows:

Ion Source and "Wehnelt"	~	100 kV
Extractor and Tube no. 1	~	90 kV
Tube no. 2	~	0 kV

For a better understanding of the behavior of ions in such an ion optical system calculations of ion trajectories were carried out.

For a rotational symmetric geometry the electrostatic potentials were calculated using the "relaxations method" as described, for example, by Paszkowsky /7/. The potentials are determined by iteration at the grid points of a matrix of 120x60 points keeping the potentials on the electrodes constant. Electrodes with slopes different from 0° or 90° can be approximated only by steps. Electrical fields calculated from such "step-potentials" are reliable only if the grid points are very close to each other. This in turn requires very long computer times. Ion trajectories in the regions of step-approximated-electrodes therefore must be considered carefully. The ion paths in the potentials determined as described above are calculated taking into account space charge effects resulting from an ion current density having a Gauss distribution with a maximum intensity of 3 mA/cm^2.

Fig. 3 shows ion trajectories in an electrode system geometrically similar to the one of our gun. The slopes of the "Wehnelt" and the extractor are approximated by steps as shown. The electrical fields in this region and therefore the trajectories differ from reality. The entrance conditions of the ions into the lens region (of the two tubes) are consequently different from the experiment. In addition, in the calculation the ions are assumed to start equally spaced on the ion source. In reality, however, it cannot be excluded that one part of the emitter, e.g. the center, contributes much more to the beam than others.

In this calculation the divergence of the trajectories was minimized. The resulting extraction potential does not agree with the experimental one; but, as mentioned above, in the extractor-region the calculation is expected to differ most from the experiment. Nevertheless, it is possible to learn some interesting details about the ion trajectories: In all of the calculations with various geometries and with different potentials the trajectories never crossed the center line, i.e. there is no real focal point. Furthermore, in all calculations the trajectories came more or less close to each other in the region between the tubes and diverged afterwards. The angle of divergence can be influenced by the length of the tubes and by the distance between them, as well as by their potential difference.

It has to be pointed out that it is not possible to determine the divergence of the real ion beam by just taking the outermost trajectories of the calculation , because the emitting pattern of the surface of the ion source is unknown.

2.3 THE NEUTRALIZER

The neutralizer /8/ consists of a reservoir in which the charge-exchange medium (lithium or sodium) is evaporated and a neutralization tube in which the neutralization takes place. The reservoir and neutralization tube are separated by a pneumatically-driven valve which is opened about 1 sec before the high voltage is applied to the accelerator-system (Fig. 4).

At energies higher than 10 keV the charge exchange cross section for the process $Li^+_{fast} + Na_{slow} \rightarrow Li_{fast} + Na^+_{slow}$ is greater than for the process $Li^+_{fast} + Li_{slow} \rightarrow Li_{fast} + Li^+_{slow}$ /9/. Moreover using sodium has the advantage that the neutralizer reservoir has to be heated to only about 220°C instead of about 400°C as in the case of lithium.

2.4 THE MECHANICAL SET-UP

The above described ion source, accelerating system and neutralizer are installed in a vacuum system (pressure ~ 10^{-6} mbar) as shown in figure 5. In order to prevent sparking to adjacent structures the HV-part of the vacuum system is mounted in a high pressure vessel filled with about 3 bar SF_6. SF_6 has the property of a high quality insulator. (At pressures above 3 bar SF_6 is a better insulator than transformer oil) /10/.

The ion source and the "Wehnelt"-cone are mounted on a flange by 10 keV-insulators. For optimization purposes the flange, and thus the ion source with the "Wehnelt", can be moved with respect to the extractor cone by means of a bellows. The first tube is attached to the extractor. The second tube can be moved with respect to first with the help of a rotation feed through. The two tubes are electrically insulated from each other by a ceramic tube of 150 mm ø and 90 mm length. The ion beam is extracted from the emitter by the extractor (ΔU ~ 10 kV), then accelerated and focussed by the voltage between the two tubes (ΔU ~ 90 kV). After passing the second (grounded) tube it can be steered slightly by two pairs of deflection plates (length: 100 mm; separation between plates: 60 mm). Because of the spatial restrictions on W VII-A the two pairs of deflection plates are situated in the same plane perpendicular to the direction of the beam. The ion beam is neutralized in the charge-exchange cell. Residual ions are removed by a deflection magnet.

2.5 THE DETECTOR

The detector is a combined Faraday-cup/secondary-electron detector. It consists of three elements (Figure 6). The collector is made of molybdenum and is mounted at an angle of 45° to the direction of the beam. A cylinder, its axis parallel to the axis of the beam, surrounds the collector. A disc with an entrance hole of 5 mm ø is placed in front of this cylinder. The whole setup is surrounded by a grounded box in order to prevent electrical disturbances.

The detector is calibrated with the ion beam (neutralizer turned off): The disc is kept at a potential of -300 V, which prevents secondary electrons from escaping. The total current brought to the collector and the cylinder is measured. The detector then works as a Faraday-cup.

If both the disc and the cylinder are kept at a positive potential of +300 V, then these electrodes extract all of the secondary electrons from the collector. The collector current then measures the secondary electron signal and the direct ion current. This signal minus the ion current yields the secondary electron current. This compared to the ion current (Faraday-cup), yields the secondary electron emission coefficient.

Since at energies as high as 100 keV the secondary electron emission coefficients for ions and neutral particles of the same species are the same, the detector is also calibrated for neutral particles. The number of neutral particles per cm^2 and second is calculated by dividing the secondary electron detector signal by the secondary electron emission coefficient.

It should be mentioned that by changing the condition of the collector surface, e.g. by venting the vacuum system or by heating the detector, the secondary electron emission coefficient is changed. The calibration then has to be repeated. Depending on the condition of the collector surface the secondary electron emission coefficient for a lithium beam of 100 keV is of the order of 5-7.

3. RESULTS

As mentioned above, the aim of the development was to produce a neutral lithium beam with energies up to 100 keV with intensities as high as possible at a distance of about 210 cm between the neutralizer and detector - this distance corresponding to the separation between the source and the torus of W VII-A.

Figure 7 shows the spatial distribution of the beam intensity in two perpendicular directions (called x and y): the peak intensity of the beam is equal to $1.94 \times 10^{16} sec^{-1} cm^{-2}$, the FWHM's are 1.25 cm in x-direction and 0.8 cm in y-direction. This corresponds to an equivalent current of about 2 mA in an area of 1 cm^2.

These results were obtained under the following (optimized) conditions:

Distance between emitter and extractor	16	mm
Distance between tube 1 and tube 2	66	mm
Extraction voltage	9.9	kV
Acceleration voltage	87	kV
Total beam energy	96.9	keV
Steering voltages at the x/y-deflection-plates	-150 V/-300	V
Extracted current from the HV power supply	~ 6	mA

The difference in the FWHM's of the beam in the x- and y-directions results from the different voltages across the x/y-deflection plates which creates an asymmetry of the electrical field.

In the following parameter study of beam intensity each parameter is varied one at a time, all other parameters being kept constant at the "optimum" values given above. Fig. 8 shows the dependence of the beam peak intensity on the extraction voltage.

A sharp peak in the intensity is to be seen at $U_{Extr.} = 9.9$ kV. The intensity grows slowly from 6.0 to 8.5 kV with intensities of less then 10 % of the peak intensity, it grows faster from 8.5 kV to 9.9 kV and drops again at higher voltages.

The dependence on the distance between emitter and extractor is shown in Figure 9. It is not as strong as the dependence on the extraction voltage, but there exists an optimum distance at 16.8 mm. For these conditions it is not possible to lower the distance below 16.0 mm because of the danger of HV sparking.

Fig. 10 shows the dependence on the distance between the two acceleration tubes. Also in this case the distance could not be decreased below 60 mm, because of HV sparking. The optimum distance is about 66 mm.

Fig. 11 shows the steering effects of negative voltages across the deflecting plates, maintaining the detector at a fixed position. It is to be seen that a slight spatial displacement probably resulting from misalignment of the beam line can easily be corrected by applying the proper voltages to the deflection plates. The influence, however, of the plates is more complex: if the deflection voltage is negative and the opposite plate is grounded, then this negative net voltage across the plates results in a drastical drop of the current drawn from the ion source HV power supplies from about 20 mA or more to values of about 6 mA. The negative net voltage produces a potential barrier for electrons downstream in the beam, preventing them from hitting the ion source, and thus increasing the drawn current. A positive voltage across the deflection plates does not reduce the current drawn from the HV power supplies.

In our case, the effects of the potential barrier and the deflection cannot be separated. In a setup with fewer spatial restrictions the x- and y-deflection plates should be situated behind each other. A separate aperture or short tube kept on a negative potential could produce the potential barrier.

In a different run the intensity distribution not only in the directions of x and y, but also in those of $y = 1.25x$ and $y = -1.25x$ were measured. The results are plotted in a contour-diagram (Figure 12). The respective FWHM are:

$y = 0$,	x-direction:	FWHM = 1.00 cm
$x = 0$,	y-direction:	FWHM = 1.25 cm
$y = 1.25x$-direction:		FWHM = 1.00 cm
$y = -1.25x$-direction:		FWHM = 1.30 cm

In Fig. 13 the measured intensity distribution of a 97 keV-beam is compared to a Gauß-function. The measured intensity is normalized to unity and has a FWHM of 8.5 mm. The dashed curve is a Gauß-function with a FWHM of 8 mm. This function folded with a box-function of 5 mm width, corresponding to the opening of the detector, is shown as a solid curve.
It is to be seen that the measured distribution of the beam can nicely reproduced by a Gauß-function.

SUMMARY

A gun producing a neutral lithium beam with energies up to 100 keV has been developed. The ion beam is formed by extracting lithium ions from a solid ion source and accelerating and focussing them in an electrostatic two-tube system. This ion beam is neutralized in a charge-exchange cell. The ion beam has to be carefully optimized by varying extraction- and accelerating-voltages as well as the distances between ion source and extractor and between the two tubes. A negative net voltage across the deflection plates forming a potential barrier for electrons in the beam drastically lowers the current drawn from the HV power supplies. At the same time the beam can be steered by these voltages. Calculations carried out for a potential distribution similar to the experimental one show that the ions have a narrow spatial distribution between the tubes and diverge afterwards.

An optimized neutral beam with an energy of 100 keV at a distance of 210 cm from the neutralizer has a peak particle flux density of $2 \times 10^{16}\,\mathrm{sec}^{-1}\mathrm{cm}^{-2}$ ($\hat{\approx}$ 3 $\mathrm{mA/cm}^{-2}$) and a FWHM of 0.8 cm.

The peak intensity of the beam depends strongly on the optimization of the ratio of the applied voltages and the different distances as well as on the extracted ion current, i.e. on the condition of the ion source.

REFERENCES

/1/ K. McCormick, M. Kick and J. Olivain,
Proceedings of the Eighth European Conference on Controlled Fusion and Plasma Physics, Prague, 1977, 140

/2/ K. McCormick, IPP Laborbericht, 1978, IPP III/40

/3/ J.P. Blewett and E.J. Jones, Phys. Rev. 50, 1936, 465

/4/ W. Möller and D. Kamke, Nucl. Instr. and Methods, 105, 1972, 173

/5/ O. Heinz and R.T. Reaves, Rev. of Scient. Instr., 39, 8, 1968, 1229

/6/ Pierce, Theory and Design of Electron Beams, D. Van Nostrand Company, N.Y., 1954, 173

/7/ Paszkowski, Electron Optics, Iliffe Books Ltd., 1968, M. v. Ardenne, Tabellen der Elektronenphysik, Ionenphysik und Übermikroskopie, I. Band, VEB Verlag der Wissenschaften, Berlin, 1956

/8/ K. McCormick, IPP Laborbericht, 1983, IPP III/82

/9/ H.S.W. Massey, E.H.S. Burhop and H.B. Gilbody, Electronic and Ionic Impact Phenomena, sec. Ed. Vol. IV, The Clarendon Press, Oxford, 1974, 2798

/10/ Kali-Chemie, Druckschrift: KC-Schwefelhexafluorid (SF_6)

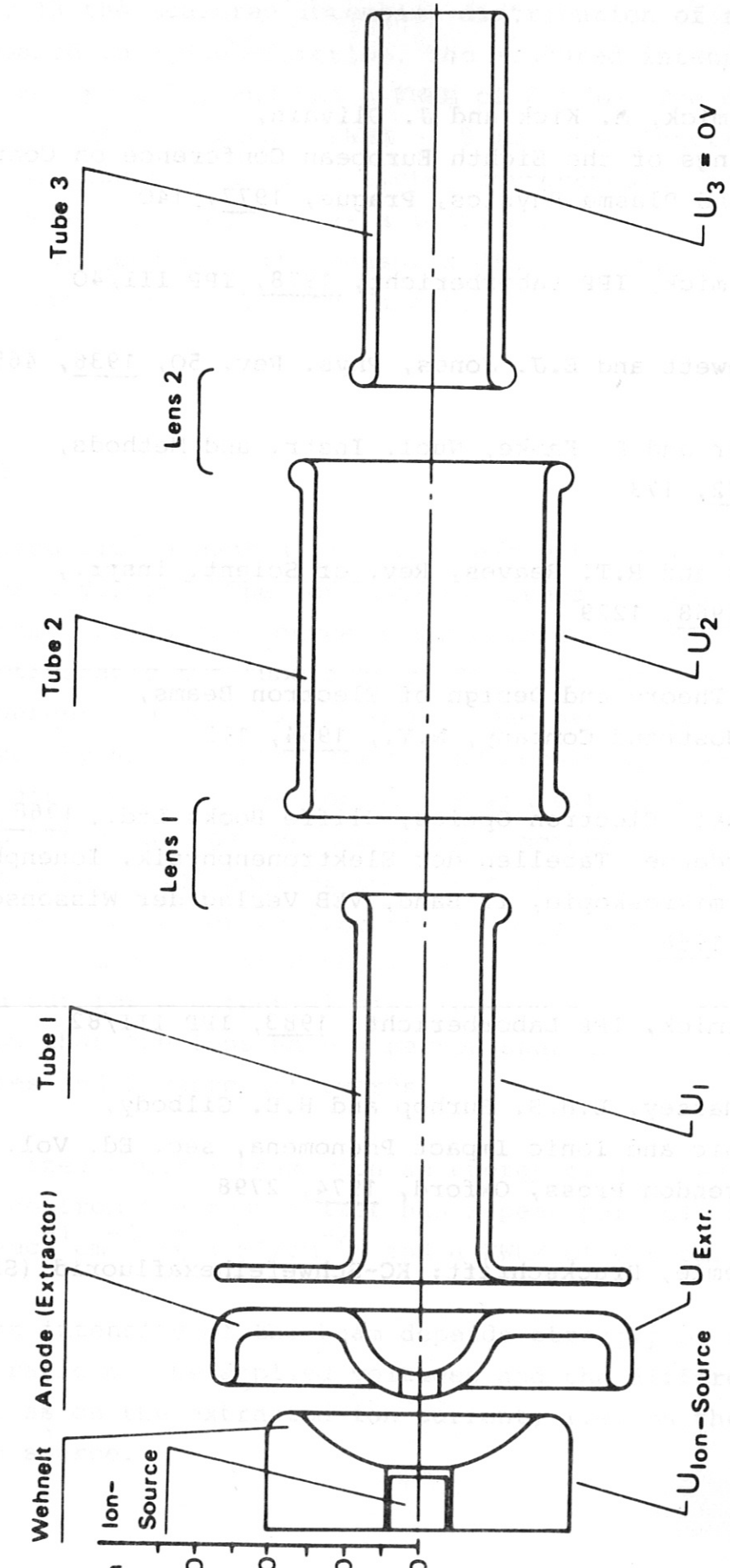

Fig. 1: Ion optical system with Pierce extraction system and 3 stage acceleration system.

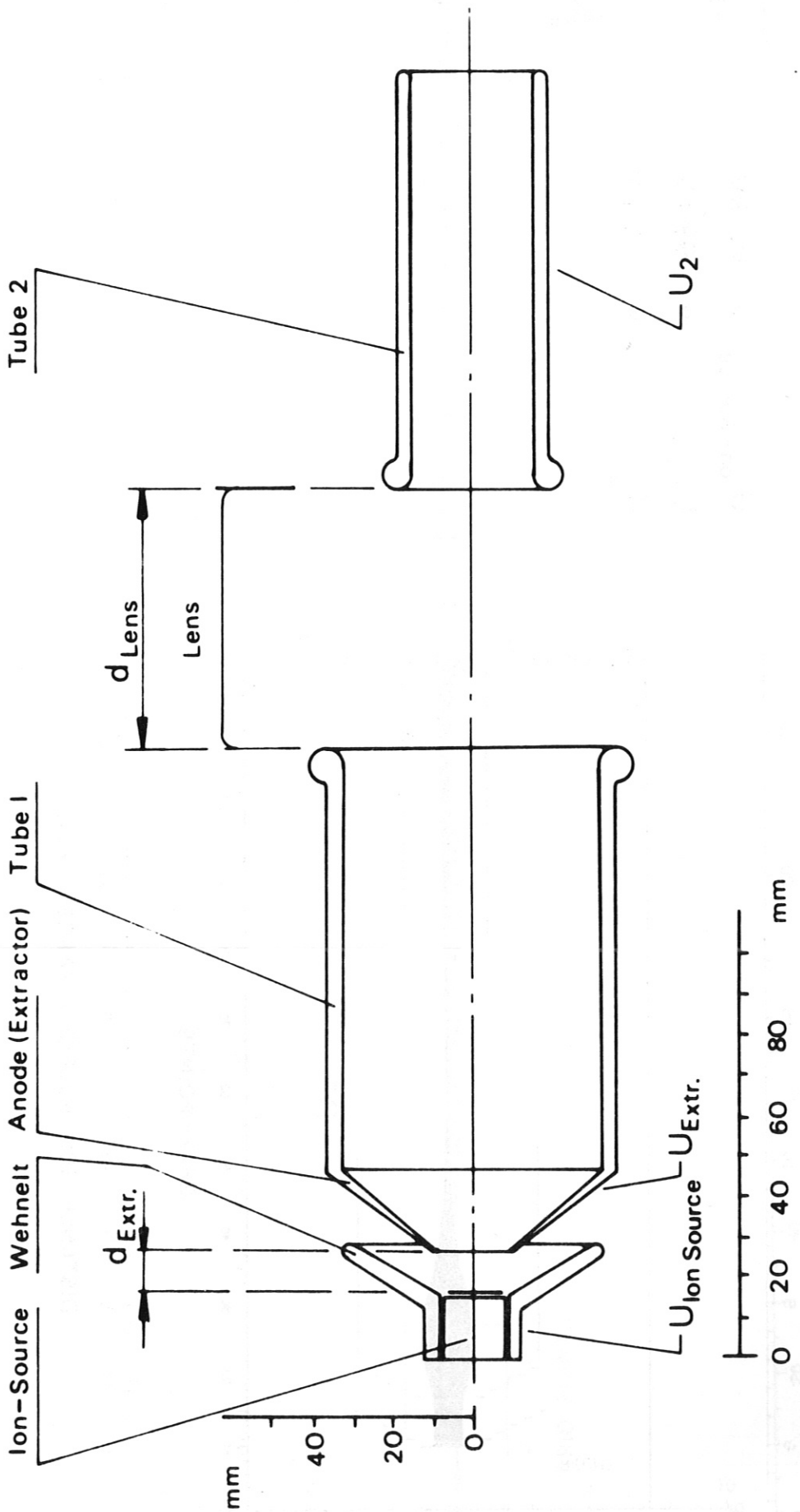

Fig. 2: Ion optical setup (optimized), immersion lens system

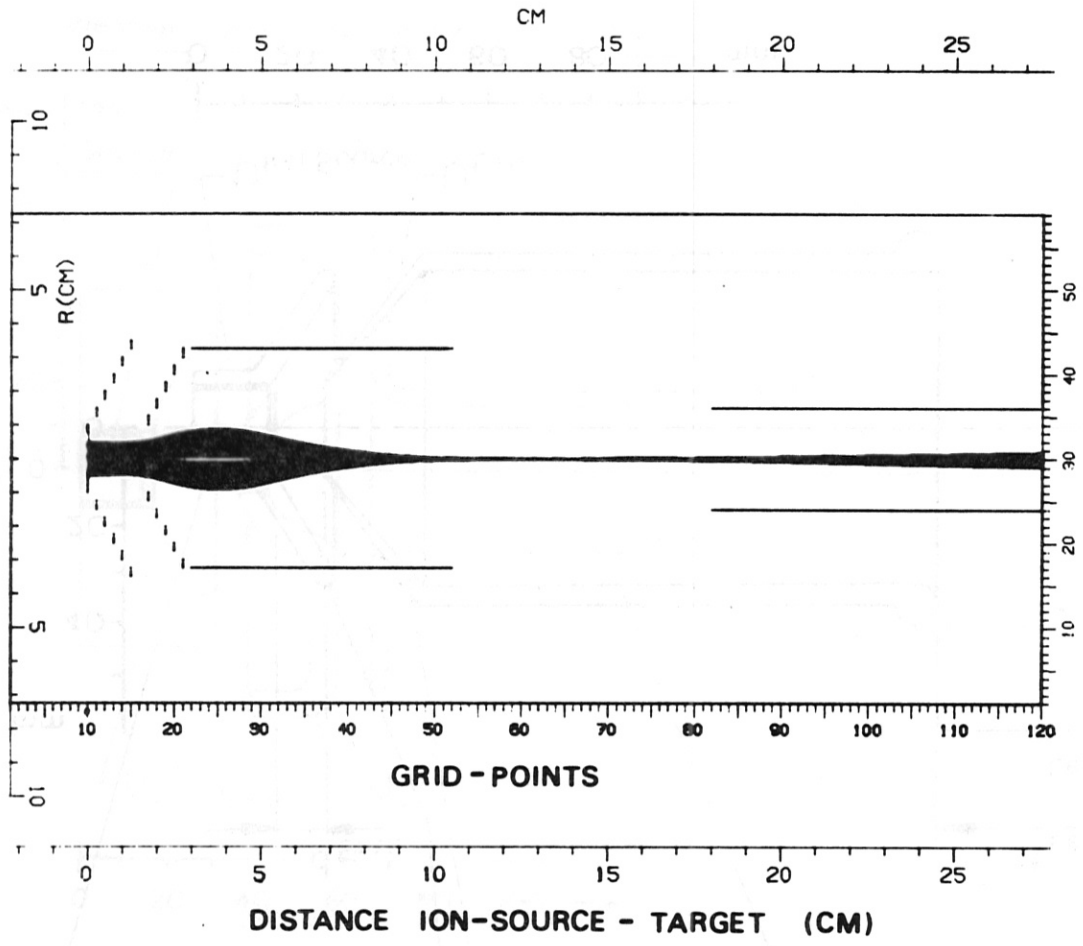

$U_{Ion-Source}$ = 100 kV

U_{Extr} = 99 kV

U_2 = 0 kV

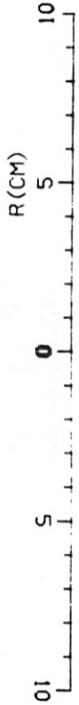

Fig. 3a: Calculated ion trajectories for the depicted ion optical system and voltage potentials.

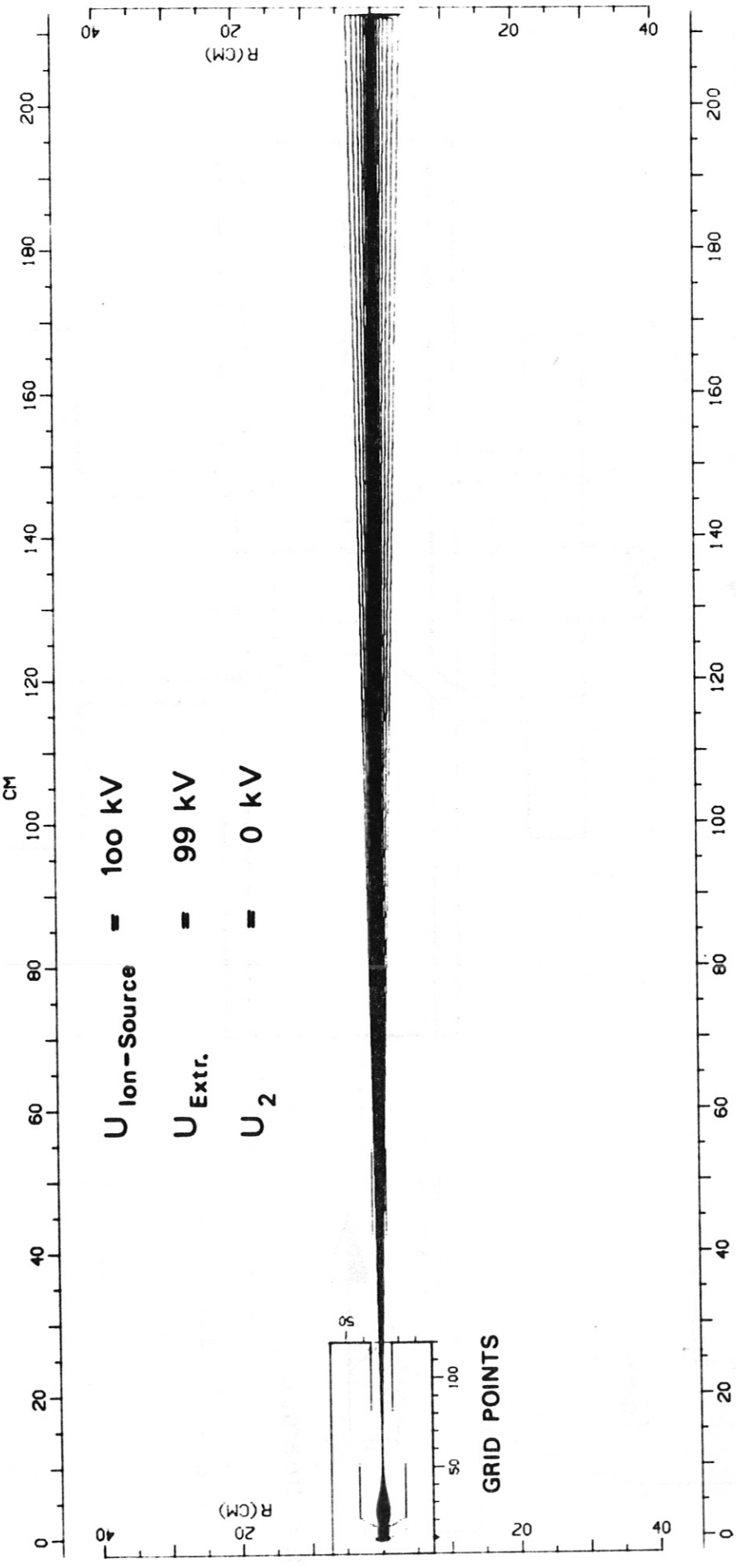

Fig. 3b: Calculated ion trajectories external to the gun for the case of Fig. 3a.

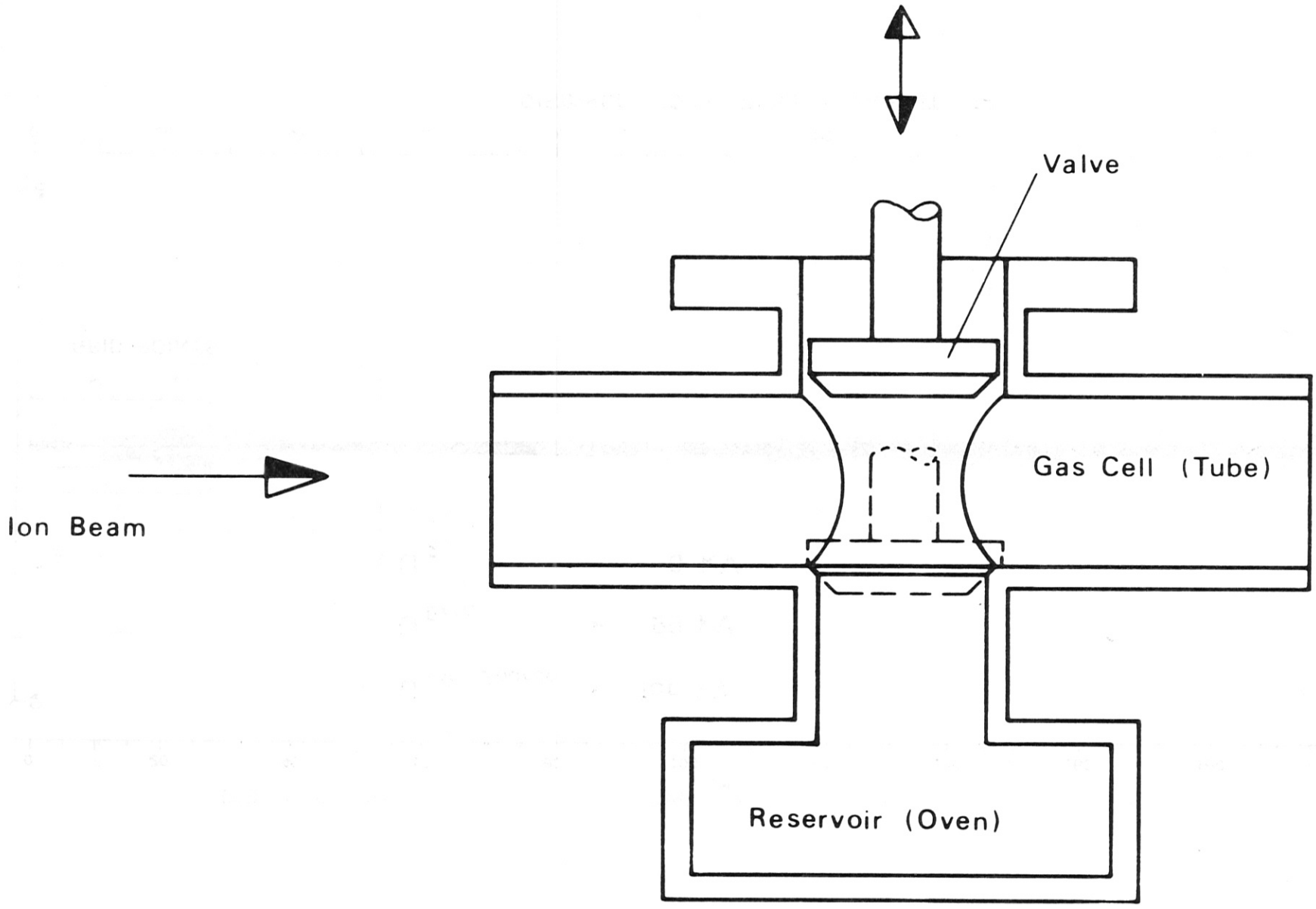

Fig. 4: Schematic of neutralizer.

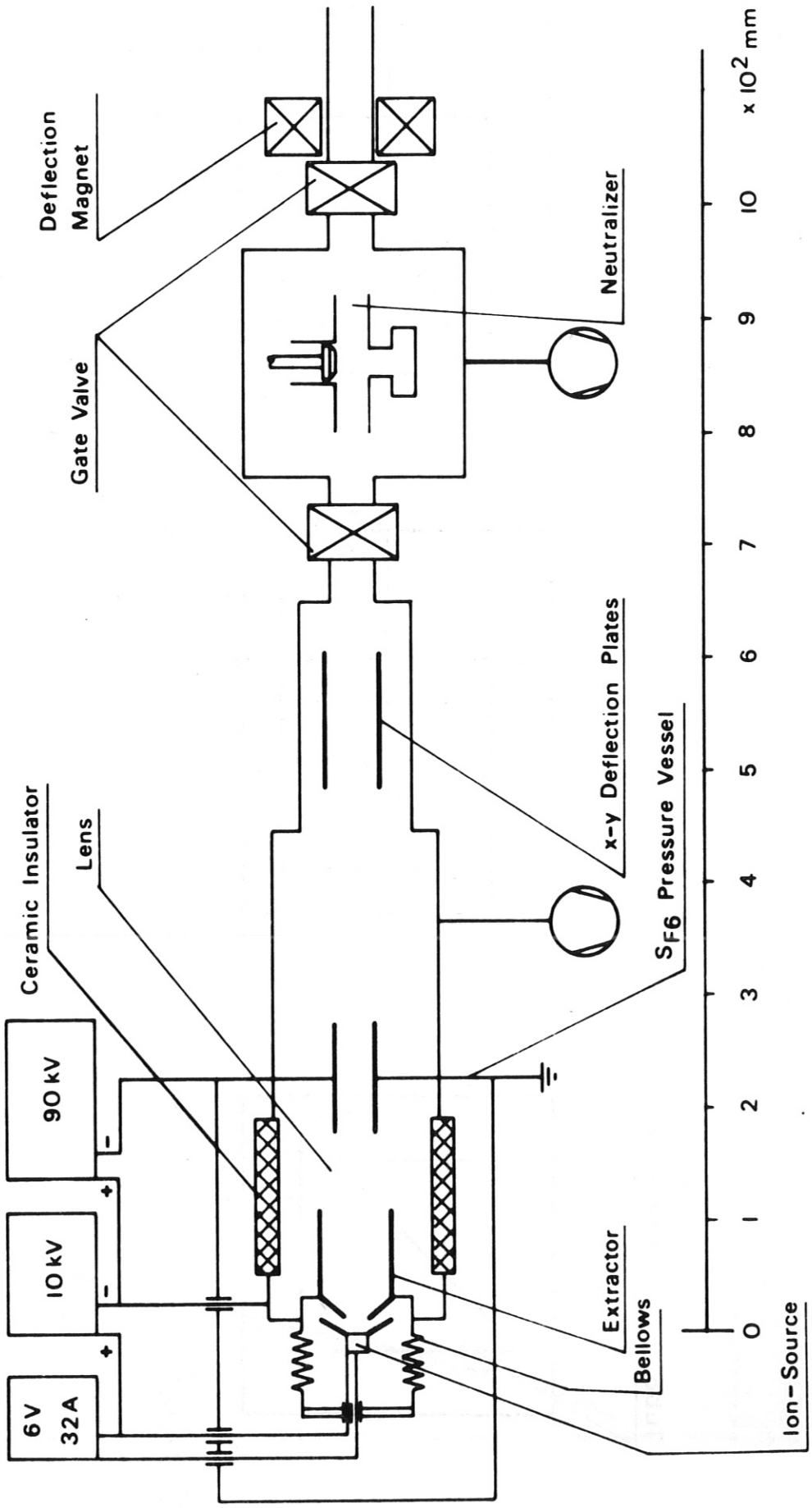

Fig. 5: Layout of the lithium gun.

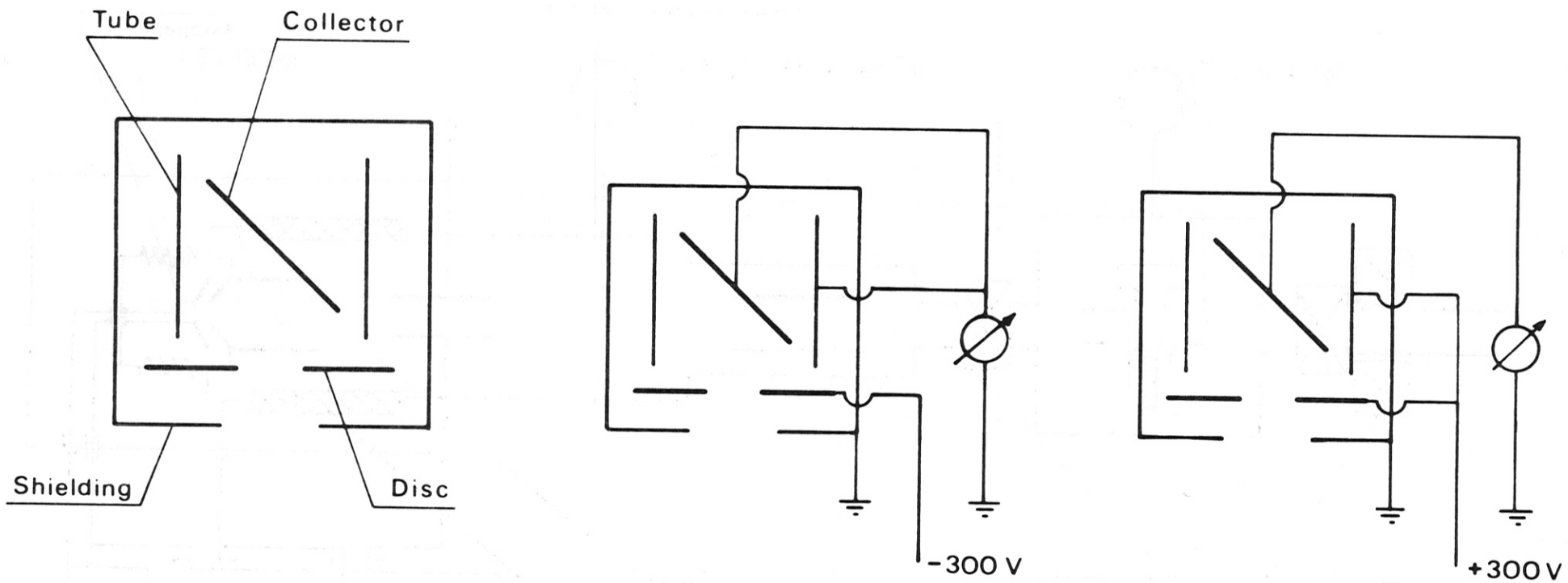

Fig. 6: Detector

a) Mechanical set up

b) Faraday cup

c) Secondary electron detector.

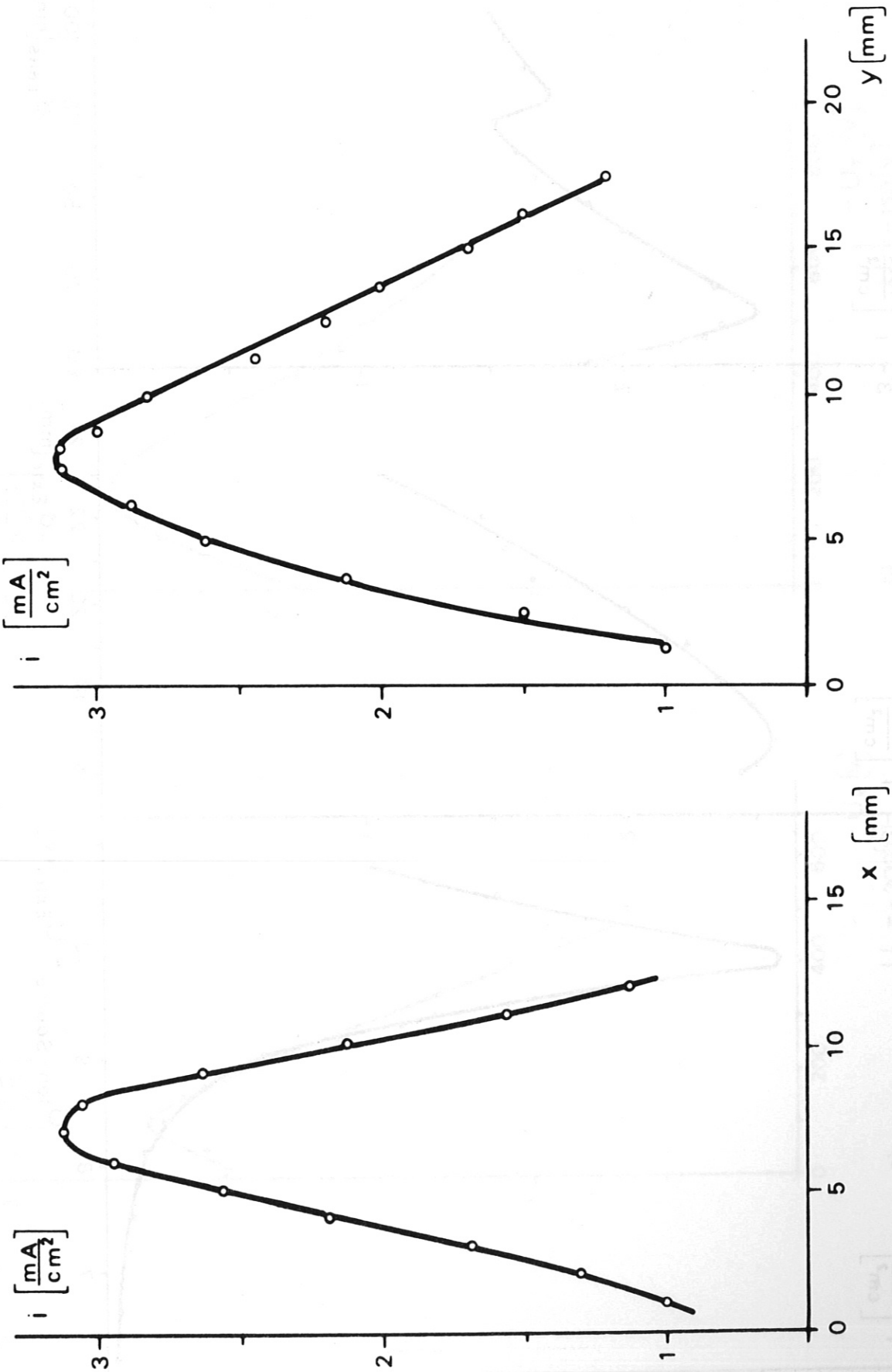

Fig. 7: Beam current density profiles.

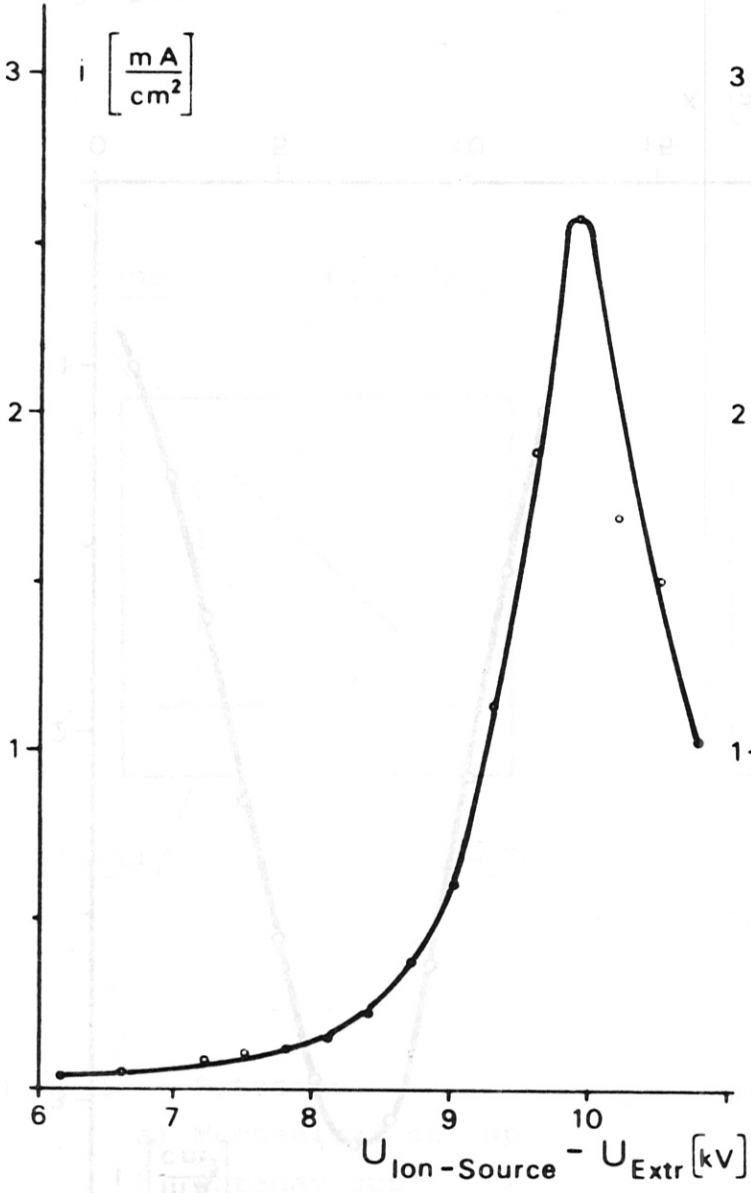

Fig. 8: Beam intensity dependence on the extraction voltage.

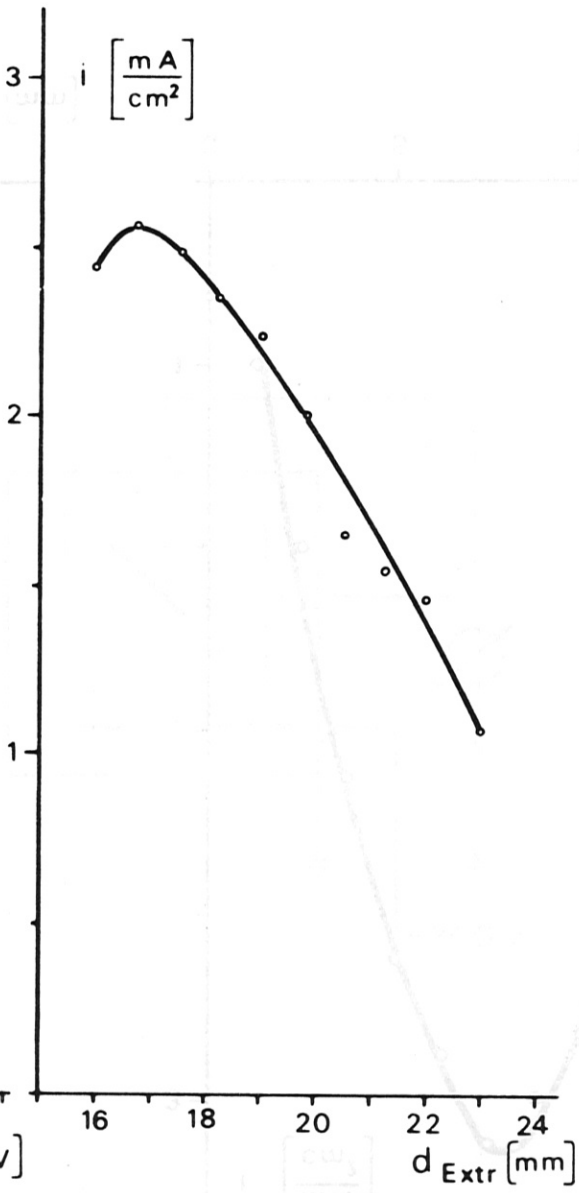

Fig. 9: Beam intensity depending on the distance between ion source and extractor.

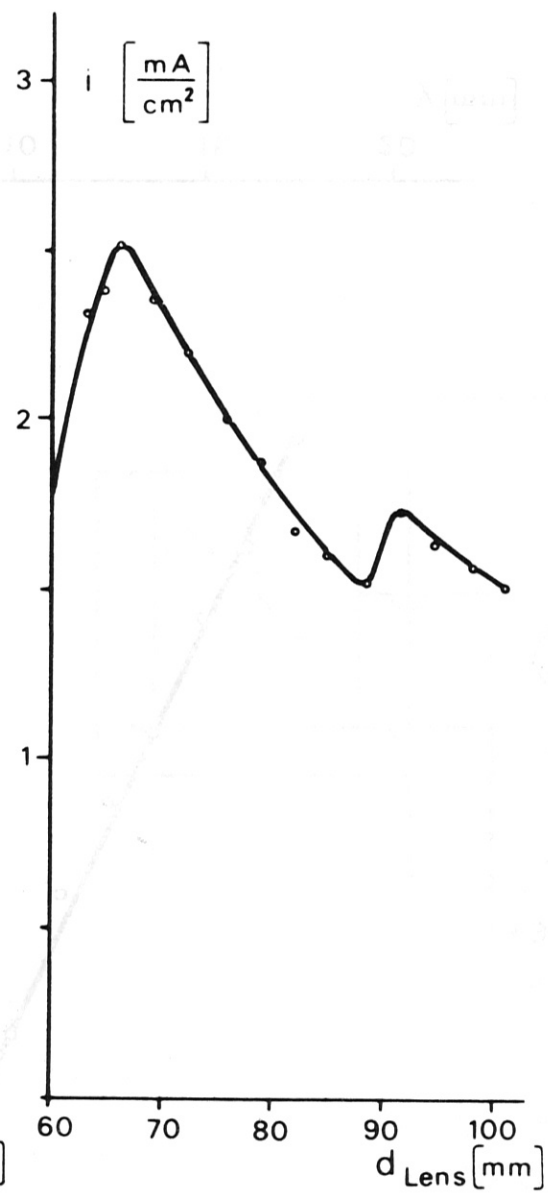

Fig. 10: Beam intensity depending on the gap between the two lens tubes.

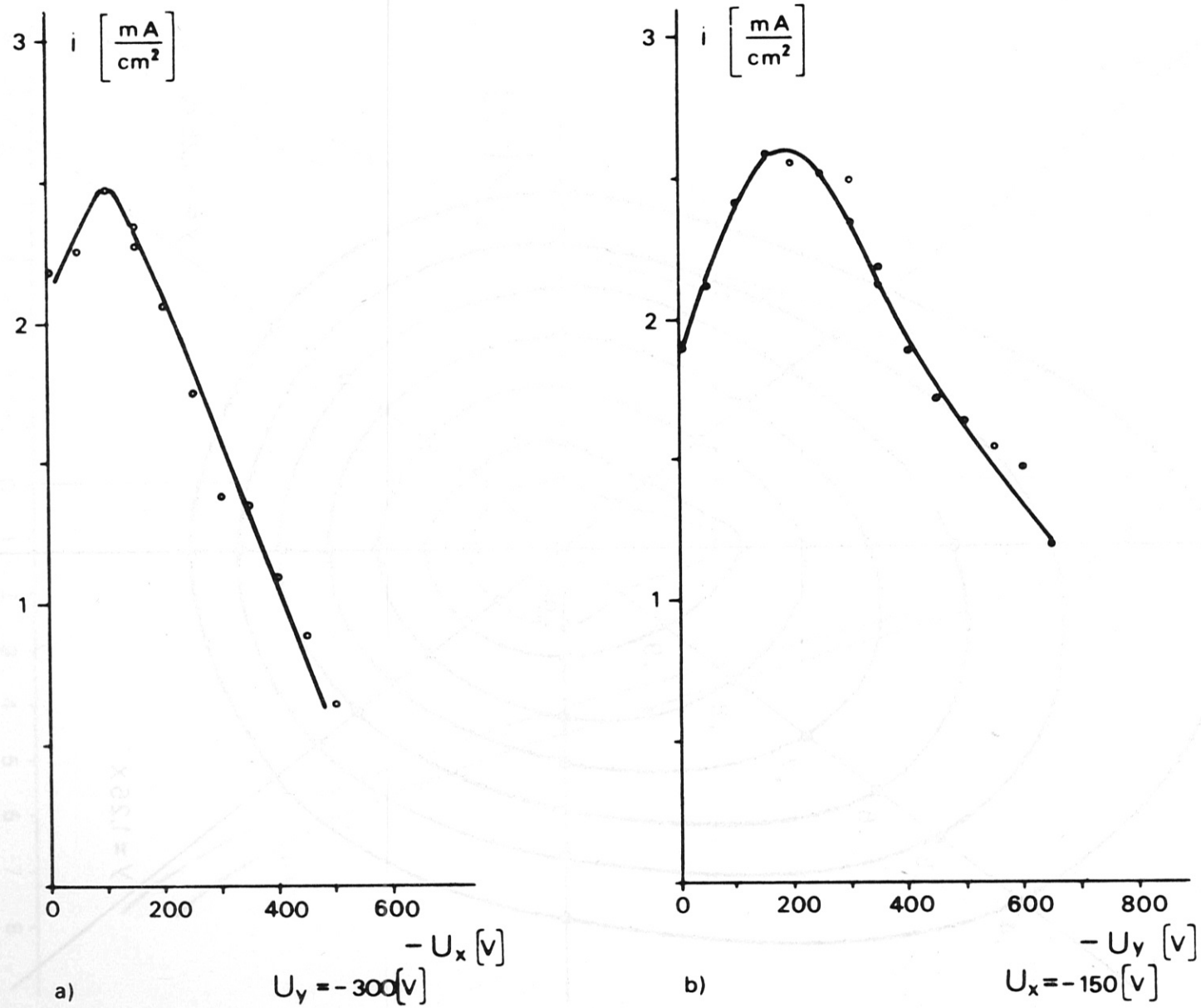

Fig. 11: Intensity of the lithium beam as a function of voltages across the deflection plates.

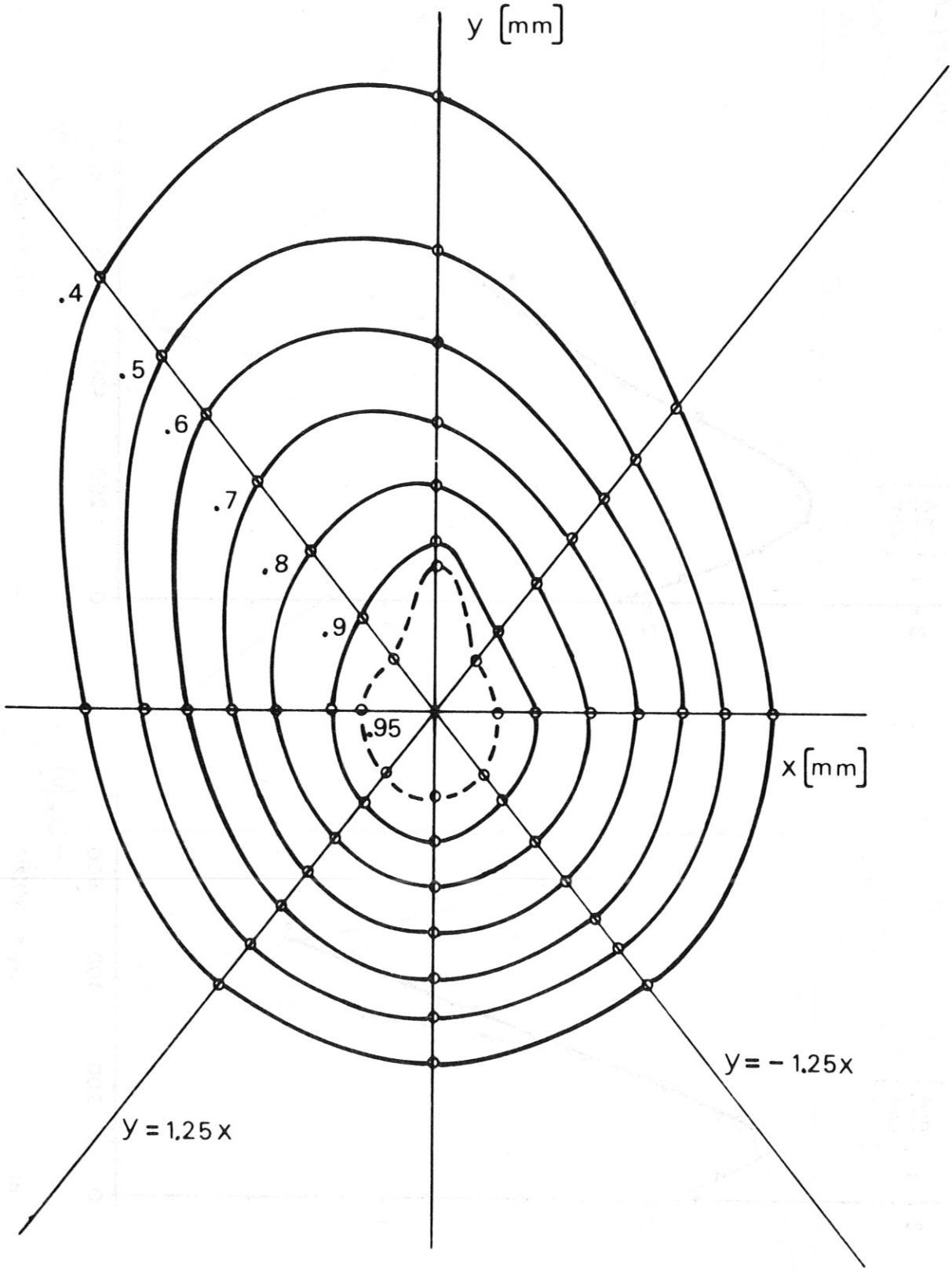

Fig. 12: Contour-diagram (normalized) of 97 keV neutral lithium beam.

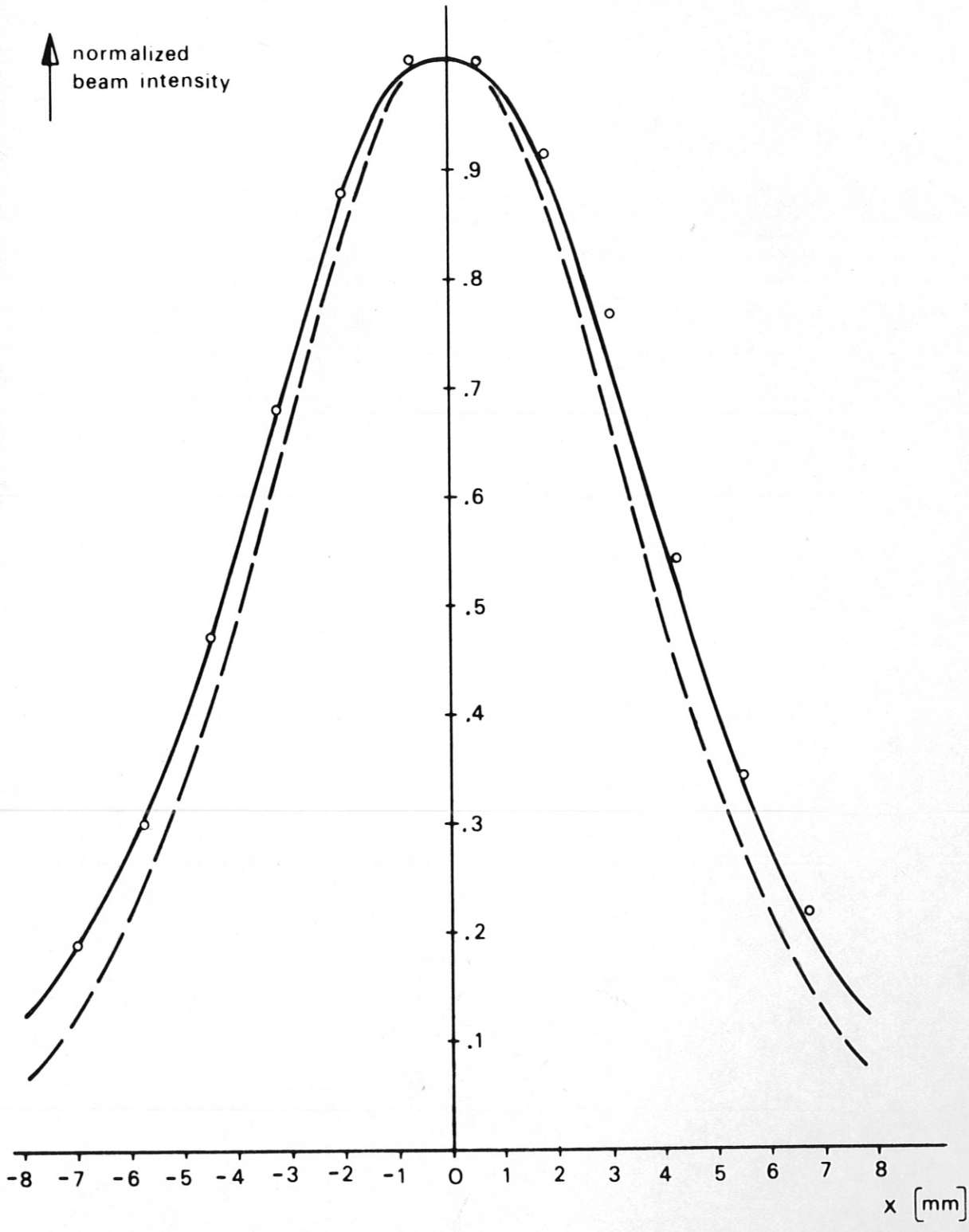

Fig. 13: Measured beam profile (open circles) compared to a Gaussian profile (dashed curve) and a Gaussian function folded by a box function of 5 mm width (solid curve).